UCRL-JC-124531
PREPRINT

Amplitude and Phase Modulation with Waveguide Optics

S. C. Burkhart
R. B. Wilcox
D. Browning
F. A. Penko

This paper was prepared for submittal to the
2nd Annual International Conference on Solid-State
Lasers for Application to Inertial Confinement Fusion
Paris, France
October 22-25, 1996

December 17, 1996

Amplitude and Phase Modulation with Waveguide Optics

S. C. Burkhart, R. Wilcox, D. Browning, F. Penko

Lawrence Livermore National Laboratory, L-490
P. O. Box 808, Livermore, Ca 94551
Phone: (510) 423-2061, FAX (510) 422-7748

ABSTRACT

We have developed amplitude and phase modulation systems for glass lasers using integrated electro-optic modulators and solid state high-speed electronics. The present and future generation of lasers for Inertial Confinement Fusion require laser beams with complex temporal and phase shaping to compensate for laser gain saturation, mitigate parametric processes such as transverse stimulated Brillouin scattering in optics, and to provide specialized drive to the fusion targets. These functions can be performed using bulk optoelectronic modulators, however using high-speed electronics to drive low voltage integrated optical modulators has many practical advantages. In particular, we utilize microwave GaAs transistors to perform precision, 250 ps resolution temporal shaping. Optical bandwidth is generated using a microwave oscillator at 3 GHz amplified by a solid state amplifier. This drives an integrated electrooptic modulator to achieve laser bandwidths exceeding 30 GHz.

KEYWORDS

amplitude modulation, arbitrary waveform generator, ICF, inertial confinement fusion, integrated electrooptics, laser bandwidth, NIF, optoelectronic, phase modulation, pulse shaping, SBS, stimulated Brillouin scattering, temporal pulseshaping, waveguide optics

INTRODUCTION

Fiber optical components are being increasingly used for functions formerly reserved for bulk electrooptical devices. In the National Ignition Facility master oscillator, the entire design is a fiber-optical system including the oscillator, phase modulator, amplification and distribution, and amplitude modulation (Fig. 1). A number of the prototype systems have already been deployed[1-3] at Lawrence Livermore National Laboratory, including the phase and amplitude modulators, and portions of the oscillator and splitter systems. Previously, the oscillator systems in Nova, Phebus, Omega, and Shiva were based upon bulk electrooptics[4,5], requiring high voltages and high-power oscillator/cavity combinations for pulseshaping and bandwidth generation respectively. The advantages are clear, with integrated electrooptics we have demonstrated the full range of pulseshaping using 5V peak drive, and 30 GHz bandwidth using less than 2 W of electrical drive.

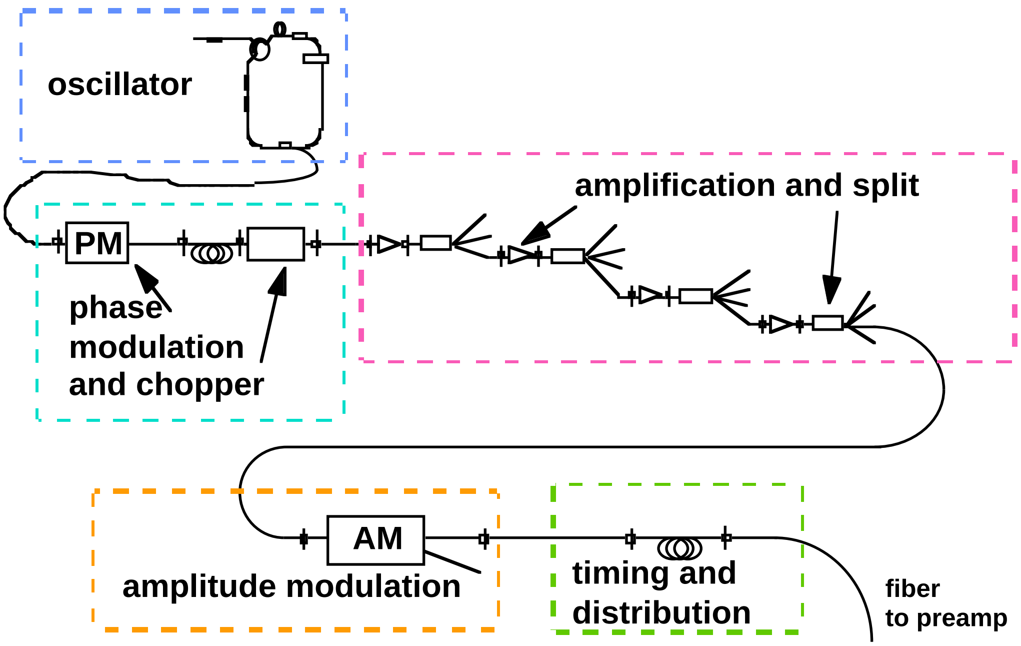

Fig. 1 The NIF master oscillator is an entirely fiber optic system, including the oscillator, phase modulation, amplification and splitting, amplitude modulation, and timing.

1. TEMPORAL PULSESHAPING

The 192 beams of the NIF laser must be precisely shaped to balance laser power on the fusion targets, demanding a readily adjustable input optical pulseshape. Experience on the 10 beamlines of Nova demonstrates the difficulty of power balance unless each beam is individually shaped, due to differing beamline losses, and variations in the amplifiers in each chain. For this reason, NIF has individual pulse shaping for each beamline cluster. Nonuniform electrical transmission lines are used[6] for arbitrary pulseshaping on Nova, Omega, and Phebus, unfortunately that approach is not amenable to computer control. Because of the lower voltage requirement, we have been able to develop circuitry based upon microwave GaAs-FET's and a high speed amplifier to produce computer controlled arbitrary electrical pulse shapes suitable for driving an integrated electrooptic amplitude modulator.

1.1 Arbitrary waveform generation - theory of operation

Arbitrary waveforms are assembled using a large number of the basic circuit section, three of which are shown in Fig. 2. Each section consists of a power GaAs-FET connected between the charged transmission line and ground, activated by the impulse from the trigger line. When 1 V of the trigger impulse is coupled to the GaAs-FET gate, it turns on, conducting current in proportion to the initial bias pulse on the gate as shown in Fig. 2b. An opposite polarity replica of the trigger pulse is generated onto the pulse line, composed of two counter propagating pulses each containing half the amplitude. The left-going pulse is absorbed by a terminator shown on the left side of figs. 2, but the right-going one becomes part of the overall shaped pulse. The amplitude of the generated pulse is dependent upon the initial bias (V_{b1}, V_{b2}, etc.), because the GaAs-FET does not turn on until the gate voltage exceeds approximately -2.2 V relative to the grounded source. If the bias is initially set to -4.0 V, the 1 V trigger pulse doesn’t turn on the GaAs-FET, and no impulse is generated on the pulse line. On the other hand, if it is initially biased at -2.2 V, it turns on strongly, making an impulse in excess of 1V. For bias voltages intermediate between these two extremes, the impulse amplitude follows a square law,

$I_{ds} \propto (V_{gs}-V_{TO})^2$ where V_{gs} = gate to source voltage due to the bias + trigger voltages, and
V_{TO} = gate cuttoff voltage (nominally -2.2 V).

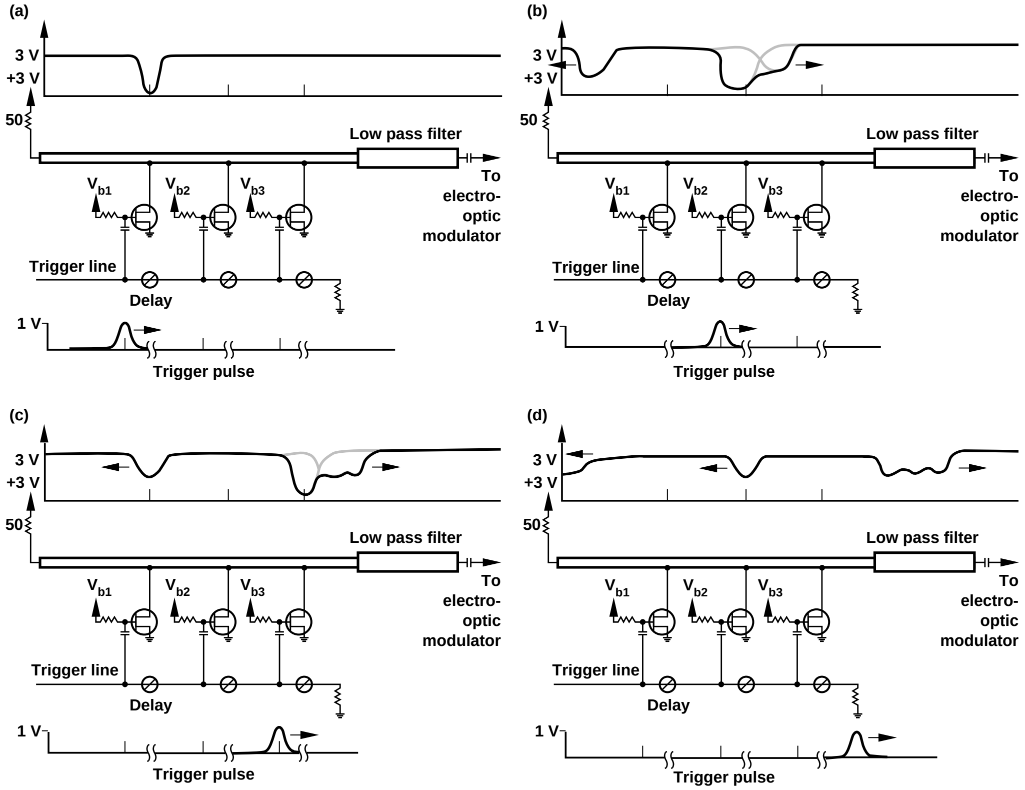

Fig 2 We generate shaped electrical pulses by adding time delayed and amplitude scaled impulses, to form the desired pulse envelope. In (a), the first impulse is launched on the pulse transmission line, and is added to in (b) and (c). The resulting square pulse from the three impulses is shown in (d). The low pass filter removes the ripple caused by the impulse addition.

Each of the elemental impulses in Fig. (2) becomes a time-slice of the overall shaped pulse. The timing between the trigger line and the pulse line are set to generate impulses at a specific rate, for our version we chose 4 giga-samples/sec (GS/s), based on an analysis of the temporal resolution required to synthesize NIF pulseshapes. For this data rate, the trigger delays shown in Fig. 2 are set to 250 ps plus the FET-to-FET delay along the pulse line. Also, the trigger pulse width is between 250 ps and 350 ps to overlap each subsequent elemental pulse onto the end of the previous one. The elemental pulses are summed as just described, with each amplitude independently set by the computer controlled gate bias voltages. The harmonics at multiples of the sampling frequency (4 GHz for our design) are suppressed by a 1.0 GHz maximally linear phase (Bessel) low-pass filter at the generator output. This constitutes a 4 GS/s arbitrary waveform generator, with a 1 GHz bandwidth, and a pulse length limited only by the number of GaAs-FETs attached to the transmission line. Presently, commercial waveform generators are limited to 1 GS/s, with a bandwidth of 200 Mhz, at a cost unacceptable to the NIF project.

1.2 Circuit realization

We tested a prototype circuit based upon Fig. 2, with 14 sections. The circuit (Fig. 3) utilizes a serpentine trigger transmission line with a 250 ps delay, and tapered to account for line and tap losses. We used a power GaAs-FET which has Vgs (max) = 15 V. The circuit board was realized using a 4-layer RT-Duroid PFTE-glass material, SMA connectors, and surface mount components.

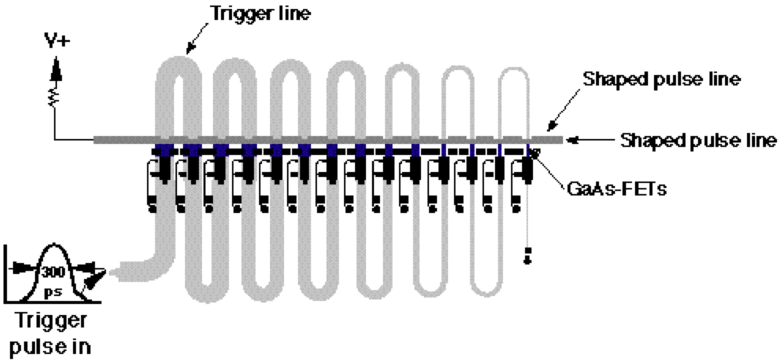

Fig. 3 View of the conductors on two of the four layers of our pulseshaping board (the other two layers are ground planes). The serpentine line is the trigger line, and the notched, straight line is where the impulses are summed into an overall pulse shape. The GaAs-FET's are mounted where the two lines cross.

1.3 Results

Two of the 14 element circuits from Fig. 3 were assembled in series and installed on the Beamlet laser system, for a total of 7 ns of shaped pulse capability. This was added to a square pulse generator to generate the 20 ns long pulses required by the NIF laser system. The combination of these systems is connected to an amplifier which drives the electrooptic modulator for optical pulseshaping. We generated overall shaped pulses to 21 ns long using this system. Future improved versions will have the full 21 ns pulse shape under computer control with a 250 ps resolution.

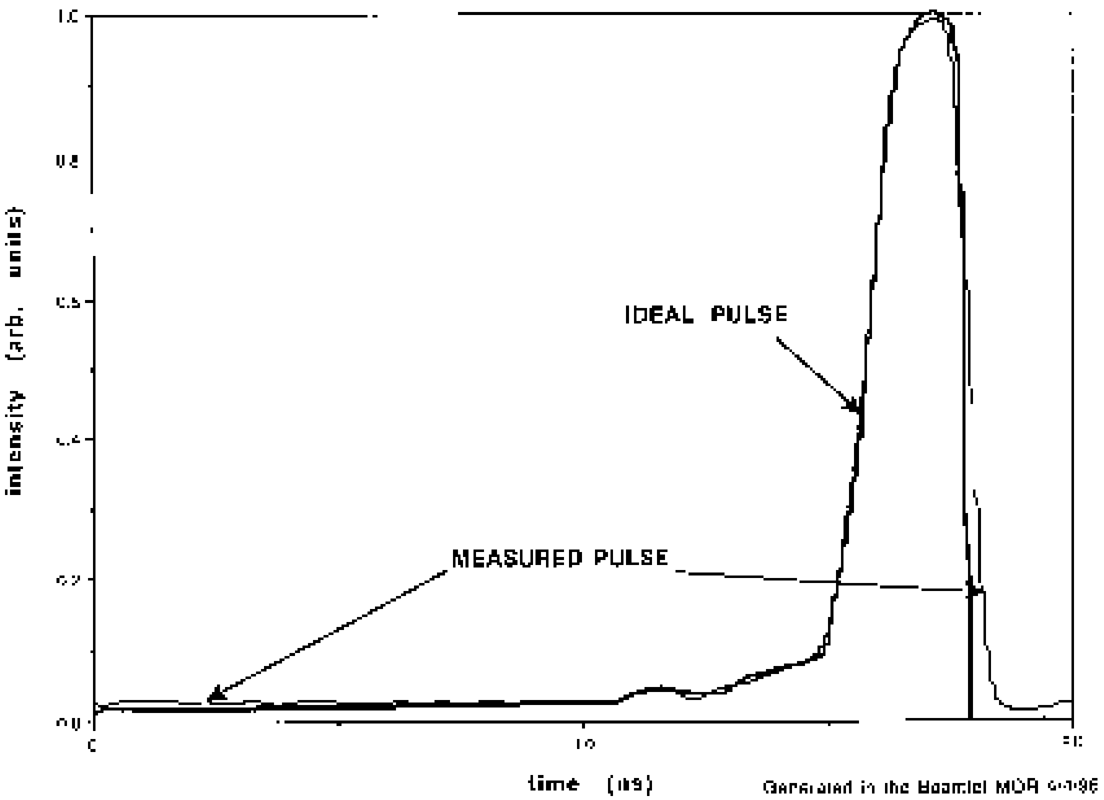

Fig. 4 Overlay plot of the optical pulse shape required for a NIF 1.4 MJ, 600 TW shot. The shaped pulse foot is formed by a square pulse generator, and the last 7 ns is generated by our arbitrary waveform system.

2.0 PHASE MODULATION

In the large optics in NIF, high laser intensity can lead to stimulated Brillouin scattering (SBS), causing catastrophic damage. To prevent this, we phase modulate the optical signal in the master oscillator room (MOR), spreading the laser energy over several wavelengths separated by more than the SBS bandwidth (approximately 1GHz). This results in several sidebands, the number of which is determined by the peak phase shift. The laser intensity-induced SBS sees the sidebands as separate frequencies, none of which is intense enough to transfer much energy into scattered light. The spacing of adjacent sidebands is exactly the modulation frequency, which we have chosen to be 3GHz to match the frequency of most of our experimental data from the Nova laser.

This phase modulation is acomplished using a waveguide electrooptic device in the circuit shown in Figure (5). A 3 GHz CW microwave oscillator is modulated by a solid state switch to produce a 2 ms microwave pulse. This is amplified in a FET amplifier and applied to the phase modulator. The amplifier is capable of 10W CW from 2 to 4 gigaHertz.

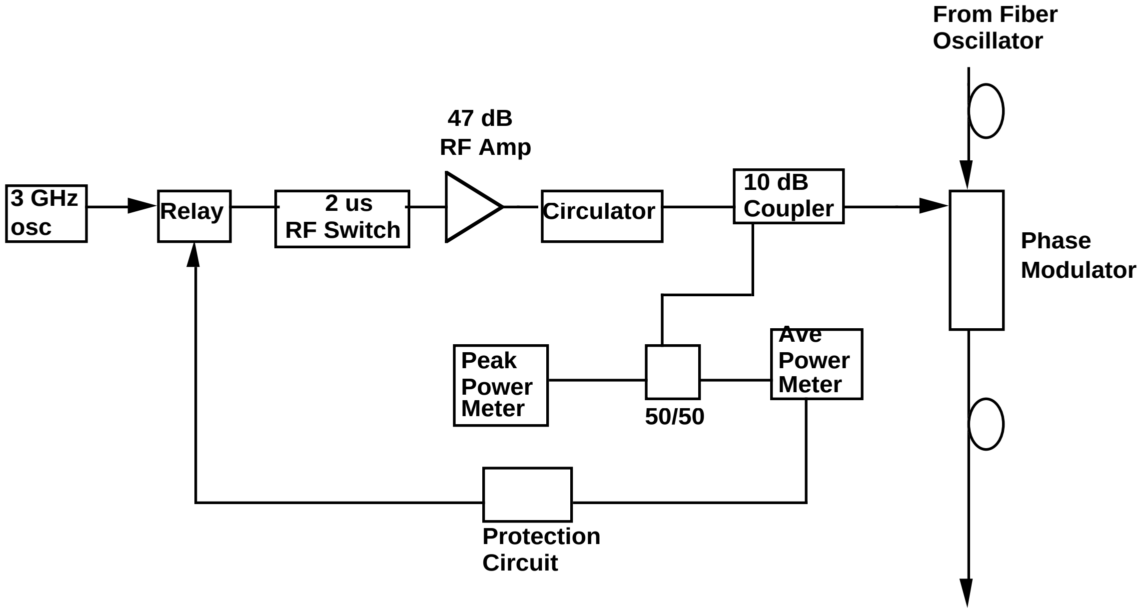

Figure 5. Phase modulation system block diagram

When a 200 ns single frequency optical pulse is passed through the phase modulator, a frequency spectrum like the one in figure 6 results. A scanning Fabry-Perot interferometer is tuned over the optical spectrum in several seconds, due to the low duty cycle (0.1 %) of the optical signal. As the etalon is slowly tuned, several pulses pass through when the tuning matches a sideband. An integrator outputs a slowly varying signal proportional to the amplitude of the pulses, so that the result can be recorded on a digital sampling oscilloscope.

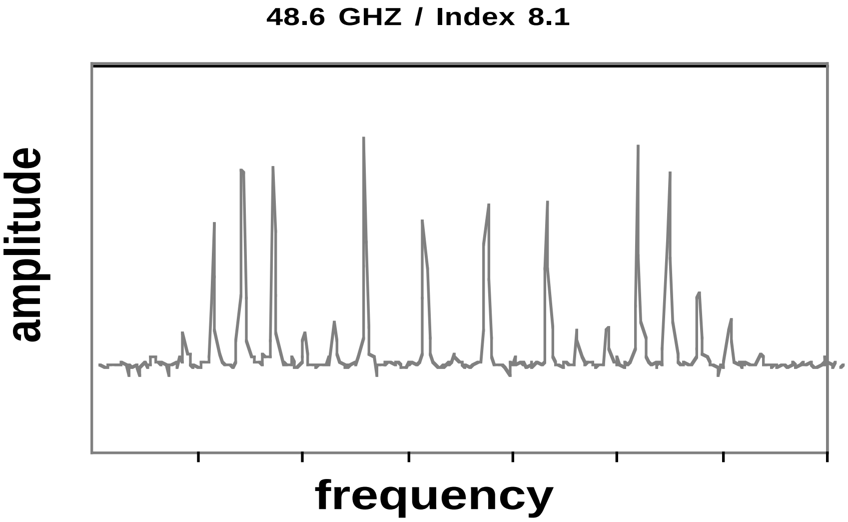

Figure 6. Sideband spectrum measured with scanning Fabry-Perot etalon.

Bandwidth can be precisely determined by comparing the measured spectra with calculated spectra. Since the power in each sideband is the square of a Bessel function with order corresponding to its position in the spectrum, the theoretical spectrum can easily be calculated, and the modulation index adjusted until the measured and theoretical spectra match. In this way we can determine the modulation depth to a few percent. The bandwidth is then twice the modulation depth times the modulation frequency.

The bandwidth is proportional to the square root of peak microwave power, as shown in figure 3. The implied half wave voltage of the modulator (5.8 volts) is close to the value measured interferometrically by the manufacturer. Only a few watts are needed to achieve the required bandwidth of 0.1 nm.

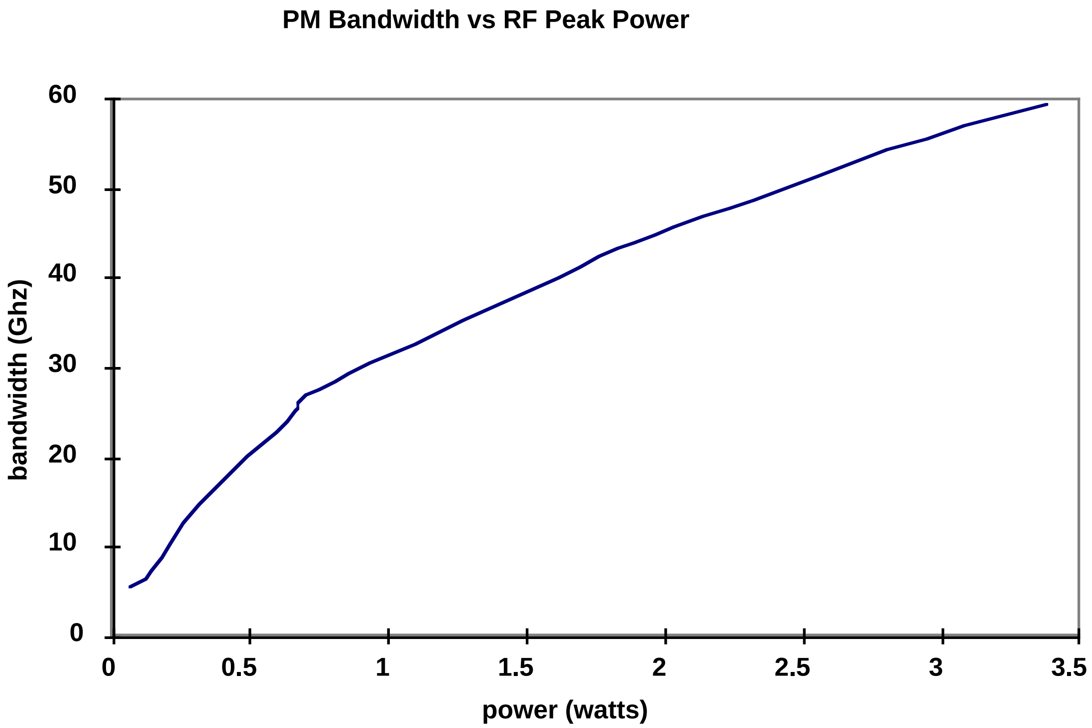

Figure 7. Optical bandwidth versus microwave peak power. The kink in the curve at 0.7 W is due to calibration error.

On NIF, there will be a detector sytem which measures the phase modulation bandwidth, and prevents passage of the pulse if the bandwidth drops below a set value.

3.0 CONCLUSIONS

The use of integrated electrooptics has been applied to meet NIF requirements for performance and cost of the master oscillator system. Temporal pulseshaping and phase modulation formatting of the oscillator pulse is demonstrated, to a precision and flexibility difficult to attain using bulk electrooptical devices. We developed specialized electronics to exploit the lower half-wave voltage of the electrooptic modulator, for high-bandwidth precision temporal pulseshaping. And we applied modern solid-state microwave electronics for precision laser bandwidth generation. These systems are continuing into the limited production required for NIF.

1. J. H. Campbell et. al., "Special Issue: Beamlet Laser Project," *ICF Quarterly Report* 5(1), pp. 42-44, Lawrence Livermore National Laboratory, Livermore, CA, UCRL-LR-105821-95-1 (1995).

2. R.B. Wilcox and D.F. Browning, "Oscillator and Pulse-Forming System for the Beamlet," *ICF Quarterly Report* 2(3), 115-122, Lawrence Livermore National Laboratory, Livermore, CA, UCRL-LR-105821-92-3 (1992).

3. R.B. Wilcox et. al., "Fusion laser oscillator and pulse-forming systems using integrated optics," *SPIE Conf. Proc.* **1870**, 53-63 (1993)

4. E. Storm, “Laser systems and operation,” *Laser Program annual report 84*, Lawrence Livermore National Laboratory, Livermore, CA, UCRL-50021-84, p 2-13

5. R. B. Wilcox, “Photoconductive switch pulse-shaping device for the Nova master oscillator,” *Lasers and Particle Beams*, Vol. 4 pp. 141-143 (1986)

6. S.C. Burkhart and R. B. Wilcox, “Arbitrary pulse shape synthesis via Nonuniform transmission lines,” IEEE Trans. on Microwave Theory Tech., Vol. 38, pp. 1514-1518, Oct 1990.

Work performed under the auspices of the U.S. Department of Energy by Lawrence Livermore National Laboratory under Contract No. W-7405-Eng-48.

Technical Information Department • **Lawrence Livermore National Laboratory**
University of California • Livermore, California 94551